OPTICAL PROPERTIES OF SMALL-RADIUS SWNTS WITHIN A TIGHT-BINDING MODEL

VALENTIN N. POPOV
Sofia University, Faculty of Physics
5 James Bourchier Blvd, BG-1164 Sofia, Bulgaria

Abstract

The optical properties of single-walled carbon nanotubes (SWNTs) are studied within a symmetry-adapted density-functional-theory-based non-orthogonal tight-binding model using 2*s* and 2*p* electrons of carbon. The use of symmetry-adapted model for the calculation of the electronic band structure and the optical properties allows reducing significantly the size of the matrix electronic eigenvalue problem. Consequently, it could be possible to do these calculations for all 48 SWNTs with radii between 2 Å and 5 Å. The obtained band structures for several nanotube types agree well with ab-initio results up to ~ 3.5 eV above the Fermi energy. Similarly to the ab-initio calculations, the tight-binding model predicts deviations from the predictions of the band structure within the zone-folding method. It is demonstrated that, e.g., nanotube (5,0) is metallic while the zone-folding method predicts it as semiconducting. Secondly, the dielectric function for the same nanotube types is calculated within the random phase approximation for energies up to 7 eV. The peak positions of the imaginary part of the dielectric function for parallel light polarisation versus nanotube radius are illustrated on a chart.

1. Introduction

The discovery of the carbon nanotubes in 1991 [1] and the speculations about their amazing properties directed much attention to their experimental and theoretical study (for reviews, see, e.g. [2-4]). In the simplest case, a nanotube consists of a single graphitic layer, the so-called single-walled carbon nanotube (SWNT). The SWNT can be viewed as a long strip of graphene sheet rolled up into a seamless cylindrical surface and can be characterised uniquely by a pair of indices (L_1,L_2). Based on a π-band tight-binding model within the zone-folding approximation (π-TB ZFA) for the non-optimised ("rolled-up") structure, the nanotubes were predicted to be metallic (zero-gap semiconductors) if L_1–L_2 is a multiple of 3 or semiconducting else [5]. It was also shown that extending this model to encompass σ and π bands, some metallic nanotubes are very-small-gap semiconducting nanotubes [5]. The predictions of such π-band tight-binding models for the optical transitions energies has been widely used for assignment of the peaks in the optical absorption spectra of nanotube samples [6]. Recently, a π-tight-binding model with a chirality- and diameter-dependent nearest–neighbour hopping integral was used to relate well resolved features in the UV-VIS-NIR spectra of

individual SWNTs to electronic excitations in specific tube types [7]. Using a non-orthogonal σ- and π-band tight-binding approach [8], a first-principles, self-consistent, all-electron Gaussian-orbital based local-density-functional (LDA) approach [9], and a plane-wave ab-initio pseudopotential LDA approach [10] dealing directly with the optimised nanotube structure, it was possible to study in more detail the curvature-induced σ- and π-band mixing and deviation from the sp^2 hybridisation. In particular, these effects were found to alter significantly the electronic structure of small nanotubes compared to the predictions of the π-band tight-binding model [10]. In the case of small-radius insulating SWNTs, strongly modified low-lying non-degenerate conduction band states are introduced into the band gap due to σ^*-π^* rehybridisation. As a result, the LDA gaps of some tubes are lowered by more than 50% and the tube (6,0) previously predicted to be semiconducting is shown to be metallic. Similar effects are observed in the electronic properties of carbon nanotubes with polygonised cross sections calculated within a plane-wave ab-initio pseudopotential LDA approach [11]. Recently, it was shown by extensive ab-initio LDA calculations that even for nanotubes with large radii R (5 Å < R < 7.5 Å) a shift of ~0.1 eV is predicted relative to the results of the π-TB (ZFA) [12].

The optical properties of SWNTs have been treated exclusively within π-band tight-binding models within the gradient approximation for the matrix elements of the linear momentum. The selection rules for allowed dipole transitions were first discussed by Ajiki and Ando [13] in the study of the low-energy optical absorption due to interband transitions as a probe of the Aharonov-Bohm effect. π-band tight-binding calculations of the plasmons and optical properties of carbon nanotube systems were presented by several groups [14-16]. A symmetry-adapted approach was implemented in Ref. [16]. Ab-initio calculations of the dielectric function were carried out for a (5,7) nanotube [17] and for three small-radius nanotubes, (3,3), (5,0), and (4,2) [18,19]. The π-band tight-binding models cannot reproduce satisfactory the electronic structure and optical properties of nanotubes with R < 5 Å. On the other hand, such calculations are much less computer-time consuming than within the ab-initio approaches. An alternative approach will be to use 1) a well-tuned non-orthogonal tight-binding model which reproduces fairly well the electronic structure of graphite up to ≈5 eV and 2) a symmetry-adapted approach which will allow one to handle nanotubes with a large number of carbon atoms in the unit cell [20].

Here, the results of a non-orthogonal tight-binding study of the electronic band structure and the optical properties of all SWNTs with radii in the range 2 Å < R < 5 Å are presented. First, the main relations between the structural parameters of a nanotube are introduced in Sec. II. The symmetry-adapted non-orthogonal tight-binding model is presented in Sec. III. The obtained electronic band structure and the dielectric function for three SWNTs is given in Sec. IV together with the chart of the radius dependence of the optical transition energies for all 48 SWNTs with radii between 2 Å and 5 Å. The report ends with conclusions (Section V).

2. The nanotube structure

The ideal single-walled carbon nanotube can be viewed as obtained by rolling up of an infinite strip of a graphene sheet into a seamless cylinder [5,8,21]. The seamlessness of the tube means coincidence of lattice points previously connected on the sheet by a lattice vector $L_1\mathbf{a}_1 + L_2\mathbf{a}_2$ ($\mathbf{a}_1$ and $\mathbf{a}_2$ are the primitive translations vectors of the sheet, L_1 and L_2 are integer numbers). This ideal nanotube can be specified uniquely by the pair (L_1,L_2). We recall that a two-atom unit cell can be mapped onto the entire graphene sheet by use of two primitive translation vectors. Similarly, a two-atom unit cell can be mapped onto the entire tube by use of two different screw operators. By definition, a screw operator $\{S_i|\mathrm{t}_i\}$ (i=1,2) executes a rotation of the position vector of an atom at an angle φ_i about the tube axis with rotation matrix S_i and a translation of the position vector at a vector t_i along the tube axis. Thus the equilibrium position vector $\mathbf{x}(l_1l_2k)$ of the k-th atom in the (l_1l_2)-th cell is obtained from $\mathbf{x}(k) \equiv \mathbf{x}(00k)$ as

(1) $$\mathbf{x}(\mathbf{l}_1\mathbf{l}_2k) = \{S_1 \mid \mathbf{t}_1\}^{l_1}\{S_2 \mid \mathbf{t}_2\}^{l_2}\mathbf{x}(k) = S_1^{\,l_1}S_2^{\,l_2}\mathbf{x}(k) + l_1\mathbf{t}_1 + l_2\mathbf{t}_2$$

We adopt the abbreviated notation $S_1(\mathbf{l}) = S_1^{\,l_1}S_2^{\,l_2}$ and $\mathbf{t}(\mathbf{l}) = l_1\mathbf{t}_1 + l_2\mathbf{t}_2$ and rewrite Eq. (1) in the form

(2) $$\mathbf{x}(\mathbf{l}k) = \{S(\mathbf{l}) \mid \mathbf{t}(\mathbf{l})\}\mathbf{x}(k) = S(\mathbf{l})\mathbf{x}(k) + \mathbf{t}(\mathbf{l})\,.$$

Here the vector index $\mathbf{l} = (l_1,l_2)$ labels the two-atom unit cells and k = 1, 2, labels the atoms in a given cell. In a similar way, one of the atoms in the two-atom unit cell can be mapped unto the other atom by use of a screw operation defined by the angle φ' and the translation t'.

The primitive rotation angles and the primitive translations of the two types of screw operations can be found from the translational periodicity and rotational boundary conditions

(3) $$N_1\varphi_1 + N_2\varphi_2 = 0\,,\ L_1\varphi_1 + L_2\varphi_2 = 2\pi\ ,\ N_1\mathbf{t}_1 + N_2\mathbf{t}_2 = \mathbf{T}\,,\ L_1\mathbf{t}_1 + L_2\mathbf{t}_2 = \mathbf{0}\,.$$

Here, $\mathbf{T}$ is the primitive translation vector of the nanotube. N_1 and N_2 are integer numbers determining the primitive translation vector and are given by the relations

(4) $$N_1 = (L_1 + 2L_2)/d\,,\ N_2 = -(2L_1 + L_2)/d\,.$$

Here d is equal to the highest common divisor d' of L_1 and L_2 if L_1–L_2 is not a multiple of $3d'$or d is equal to $3d'$ if L_1–L_2 is a multiple of $3d'$. From Eqs. (3) and (4) one obtains

(5) $$\varphi_1 = 2\pi N_2/N_c\,,\ \varphi_2 = -2\pi N_1/N_c\,,\ \mathbf{t}_1 = \left(L_2/N_c\right)\mathbf{T}\,,\ \mathbf{t}_2 = -\left(L_1/N_c\right)\mathbf{T}\,.$$

Here, the total number of the atomic pairs in the unit cell, N_c, is

(6) $$N_c = N_1L_2 - N_2L_1 = 2\left(L_1^2 + L_1L_2 + L_2^2\right)/d$$

The atomic position vectors can be written as $\mathbf{x}(n\mathbf{l}k) = \mathbf{x}(\mathbf{l}k) + n\mathbf{T}$, where the integer number n labels the (translational) unit cells.

A nanotube can be characterised alternatively by its radius R and chiral angle (or wrapping angle) θ which is the angle between the tube circumference and the nearest zigzag of C-C bonds, $0° \le \theta < 30°$ [5]. For the "rolled-up" structure these two quantities are given by

(7) $R = \sqrt{3\left(L_1^2 + L_1 L_2 + L_2^2\right)}\, a_{C-C} / 2\pi$, $\theta = \tan^{-1}\left(\sqrt{3} L_2 / \left(L_2 + 2L_1\right)\right)$,

where $a_{C\text{-}C}$ is the C-C bond length in graphene. The "rolled-up" structure is useful when the nanotube structure cannot be optimised as is the case with some tight-binding models of the electronic structure with fixed parameters or in dynamical models based on fixed force constants. However, in other tight-binding models with explicit dependence of the parameters on the interatomic separations and in all ab-initio models of the electronic structure, as well as in the potential-based dynamical models, one should optimise the tube structure. In the simplest case, only the bond lengths and valence angles for the two atoms in the unit cell are varied in the optimisation procedure preserving the screw symmetry of the tube. Thus as independent structural parameters can be considered R, T, φ', and t'. For the optimised structure the above relations between L_1, L_2 and R, θ will generally no longer hold.

1. The symmetry-adapted non-orthogonal tight-binding model

The electronic band structure of a periodic structure is usually obtained solving the one-electron Schrödinger equation

(8) $$\left[-\frac{\hbar^2\nabla^2}{2m} + V(\mathbf{r})\right]\psi_{\mathbf{k}}(r) = E_{\mathbf{k}}\psi_{\mathbf{k}}(r)\,,$$

where $V(\mathbf{r})$ is the effective periodic potential, $\psi_{\mathbf{k}}(\mathbf{r})$ and $E_{\mathbf{k}}$ are the one-electron wavefunction and energy depending on the wavevector $\mathbf{k}$. This equation can be solved by representing $\psi_{\mathbf{k}}(\mathbf{r})$ as a linear combination of basis functions $\varphi_{r\mathbf{k}}(\mathbf{r})$

(9) $$\psi_{\mathbf{k}}(\mathbf{r}) = \sum_r c_{r\mathbf{k}}\varphi_{r\mathbf{k}}(\mathbf{r})$$

In the tight-binding approach, the φ's are constructed from atomic orbitals centered at the atoms. Let us denote by $\chi_r(\mathbf{R(l)}–\mathbf{r})$ the r–th atomic orbital centered at an atom with position vector $\mathbf{R(l)}$ in the $\mathbf{l}$–th unit cell. Bloch's condition for the electron wave function φ of a system consisting of N unit cells is satisfied for the linear combination of χ's

(10) $$\varphi_{r\mathbf{k}}(\mathbf{r}) = \frac{1}{\sqrt{N}}\sum_{\mathbf{l}} e^{i\mathbf{k}\cdot\mathbf{l}}\chi_r(\mathbf{R(l)}-\mathbf{r})\,.$$

Equation (10) is applicable to any nanotube as well. The number of atoms in the unit cell of the nanotube can be very large leading to large-size matrix equations for the band problem.

We notice, however, that any nanotube has a screw symmetry, which allows one to use only a two-atom unit cell for the electronic problem. In this case, Eq. (10) is still valid but for the transformed χ's

(11) $$\varphi_{r\mathbf{k}}(\mathbf{r}) = \frac{1}{\sqrt{N}}\sum_{\mathbf{l}} e^{i\mathbf{k}\cdot\mathbf{l}}T_{rr'}\chi_{r'}(\mathbf{R(l)}-\mathbf{r})\,.$$

Here $\mathbf{k}=(k_1,k_2)$ is an yet undefined two-component wave vector of the tube and $T_{rr'}$ is the matrix realizing a representation of the screw symmetry group in the space of the χ's. Substituting Eq. (11) in Eq. (8), we obtain

(12) $$\sum_{r'} c_{r'}(\mathbf{k})H_{rr'}(\mathbf{k}) = E_{\mathbf{k}}\sum_{r'} c_{r'}(\mathbf{k})S_{rr'}(\mathbf{k})\,,$$

where

(13) $$H_{rr'}(\mathbf{k}) = \sum_{\mathbf{l}r''} e^{i\mathbf{k}\cdot\mathbf{l}} H_{rr''}(\mathbf{l}) T_{r''r'}(\mathbf{l}) \ , \ S_{rr'}(\mathbf{k}) = \sum_{\mathbf{l}r''} e^{i\mathbf{k}\cdot\mathbf{l}} S_{rr''}(\mathbf{l}) T_{r''r'}(\mathbf{l})$$

and

(14)

$$H_{rr'}(\mathbf{l}) = \int d\mathbf{r} \chi_r(\mathbf{R}(\mathbf{0}) - \mathbf{r}) \hat{H} \chi_{r'}(\mathbf{R}'(\mathbf{l}) - \mathbf{r}) \ ,$$

$$S_{rr'}(\mathbf{l}) = \int d\mathbf{r} \chi_r(\mathbf{R}(\mathbf{0}) - \mathbf{r}) \chi_{r'}(\mathbf{R}'(\mathbf{l}) - \mathbf{r}) \ .$$

The quantities $H_{rr'}(\mathbf{l})$ and $S_{rr'}(\mathbf{l})$ are the matrix elements of the Hamiltonian $\hat{H}$ and the overlap matrix elements, respectively.

The wave vector components k_1 and k_2 can be determined imposing the rotational boundary and translational periodicity conditions

(15) $$k_1 L_1 + k_2 L_2 = 2\pi l \ , \ k_1 N_1 + k_2 N_2 = k \ .$$

Here k is the one-dimensional wave vector of the tube ($-\pi \le k \le \pi$) and the integer number l labels the electronic energy levels with a given k (l = 0,1,…, N_c–1). From Eq. (15) we obtain k_1 and k_2

(16) $$k_1 = \left(2\pi N_2 l - L_2 k\right) / N_c \ , \ k_2 = \left(L_1 k - 2\pi N_1 l\right) / N_c \ .$$

The substitution of Eq. (15) in Eqs. (11) – (13) yields

(17) $$\varphi_{r\mathbf{k}}(\mathbf{r}) = \frac{1}{\sqrt{N}} \sum_{\mathbf{l}} e^{i(\alpha(\mathbf{l})l + z(\mathbf{l})k)} T_{rr'} \chi_{r'}(\mathbf{R}(\mathbf{l}) - \mathbf{r}) \ ,$$

(18) $$\sum_{r'} c_{r'}(kl) H_{rr'}(kl) = E_{kl} \sum_{r'} c_{r'}(kl) S_{rr'}(kl) \ ,$$

(19) $$H_{rr'}(\mathbf{k}) = \sum_{\mathbf{l}r''} e^{i(\alpha(\mathbf{l})l + z(\mathbf{l})k)} H_{rr''}(\mathbf{l}) T_{r''r'}(\mathbf{l}) \ , \ S_{rr'}(\mathbf{k}) = \sum_{\mathbf{l}r''} e^{i(\alpha(\mathbf{l})l + z(\mathbf{l})k)} S_{rr''}(\mathbf{l}) T_{r''r'}(\mathbf{l}) \ .$$

The quantities $\alpha(\mathbf{l})$ and $z(\mathbf{l})$ are given by

(20) $$\alpha(\mathbf{l}) = 2\pi \left(l_1 N_2 - l_2 N_1\right) / N_c \ , \ z(\mathbf{l}) = \left(L_1 l_2 - L_2 l_1\right) / N_c \ .$$

The set of linear algebraic equations Eq. (17) has non-trivial solutions for the coefficients c only for energies E which satisfy the characteristic equation

(21) $$\left| H_{rr'}(kl) - E_{kl} S_{rr'}(kl) \right| = 0 \ .$$

The solutions of Eq. (21), E_{klm}, are the electronic energy levels; the energy bands are labeled by the composite index lm (m = 1, 2,…). The corresponding eigenfunctions are $c_r(klm)$ apart from an omitted index labeling the degenerate eigenfunctions belonging to the same energy level E_{klm}.

The total energy of a nanotube (per unit cell) is given by

(22) $$E = \sum_{klm}^{occ} E_{klm} + \frac{1}{2} \sum_i \sum_j \phi(r_{ij}) \ ,$$

where the first term is the band energy (the summation is over all occupied states) and the second term is the repulsive energy, consisting of repulsive pair potentials between pairs of nearest neighbors. The force in α direction on atom with position vector $\mathbf{R}(\mathbf{0})$ is the sum of the band and repulsion contributions; the former is given by the Hellmann-Feynman theorem

(23) $$F_\alpha = \sum_{klm}^{occ} \frac{\partial E_{klm}}{\partial R_\alpha(\mathbf{0})} = \sum_{klm}^{occ} \sum_{rr'} c_r^*(klm) \frac{\partial \left(H_{rr'} - E_{klm} S_{rr'} \right)}{\partial R_\alpha(\mathbf{0})} c_{r'}(klm) .$$

The imaginary part of the dielectric function in the random-phase approximation is given by [22]

(24) $$\varepsilon_2(\omega) = \frac{4\pi^2 e^2}{m^2 \omega^2} \sum_{cv} \frac{2}{2\pi} \int dk \left| p_{cv,\mu} \right|^2 \delta \left(E_{kl'c} - E_{klv} - \hbar\omega \right),$$

where $\hbar\omega$ is the photon energy, and e and m are the elementary charge and the electron mass. The sum is over all occupied (v) and unoccupied (c) states. The matrix element of the momentum $p_{cv,\mu}$ in the direction μ of the light polarisation is

(25) $$p_{cv,\mu} = \langle kl'c | p_\mu | klv \rangle = \sum_{rr'} c_{r'}^*(kl'c) c_r(klv) f_\mu(ll') \sum_{\mathbf{l}r''} e^{-i(\alpha(\mathbf{l})l + z(\mathbf{l})k)} p_{r'r'',\mu}(\mathbf{l}) T_{rr''}(\mathbf{l}) .$$

Here, $f_x(ll') = f_y(ll') = (\delta_{l',l+1} + \delta_{l',l-1})/2$ and $f_z(ll') = \delta_{ll'}$ (z-axis is along the tube axis) are the conditions for non-zero matrix elements $p_{cv,\mu}$ and express the optical transitions selection rules (see [13]). From Maxwell's relation $\varepsilon = \tilde{n}^2$ ($\tilde{n}$ is the complex refractive index), the refractive index $n = \mathrm{Re}\,\tilde{n}$ and the extinction coefficient $\kappa = \mathrm{Im}\,\tilde{n}$ are readily obtained. The relations $\alpha = 2\omega\kappa / c$ (c is the light velocity in vacuum) and $R = \left| (\tilde{n} - 1)/(\tilde{n} + 1) \right|^2$ allow one to derive the absorption coefficient α and the reflection coefficient for normal incidence R.

Let us consider a single pair of v- and c-bands with maximum and minimum separated by a direct gap $E_{l'clv}$. Assuming that the matrix elements $p_{cv,\mu}$ are independent of k, it is straightforward to show that the contribution to ε_2 from these bands is given by

(26) $$\varepsilon_2 = \frac{2\pi e^2}{m^2 \omega^2} \sqrt{\frac{2m^*_{l'clv}}{\hbar^2}} \left| p_{cv,\mu} \right|^2 \frac{1}{\sqrt{\hbar\omega - E_{l'clv}}} .$$

Here m^* is the reduced effective mass for the two bands. Alternatively, for a pair of v- and c-bands with minimum and maximum separated by energy $E_{l'clv}$ one readily obtains

(27) $$\varepsilon_2 = \frac{2\pi e^2}{m^2 \omega^2} \sqrt{\frac{2m^*_{l'clv}}{\hbar^2}} \left| p_{cv,\mu} \right|^2 \frac{1}{\sqrt{E_{l'clv} - \hbar\omega}} .$$

In the general case, the graph $\varepsilon_2(\omega)$ will consist of two types of spikes close to those described by Eqn. (25) and (26). From the derivation of the latter two equations it is clear that the electron density of states (DOS) versus ω will have the same two types of spikes.

2. Results and discussion

The parameters of the non-orthogonal tight-binding model were taken from a density-functional-based study [23]. In the case of graphite, these parameters showed excellent performance in the calculation of the equilibrium lattice parameter and the cohesive energy. The tight-binding electronic structure of graphite corresponds fairly well to the ab-initio results for the valence bands and for the unoccupied bands up to ~3.5 eV above the Fermi energy. This implies that the optical properties of graphite should be

reproduced well up to about 7 eV. The same reliability region should be valid for carbon nanotubes as well.

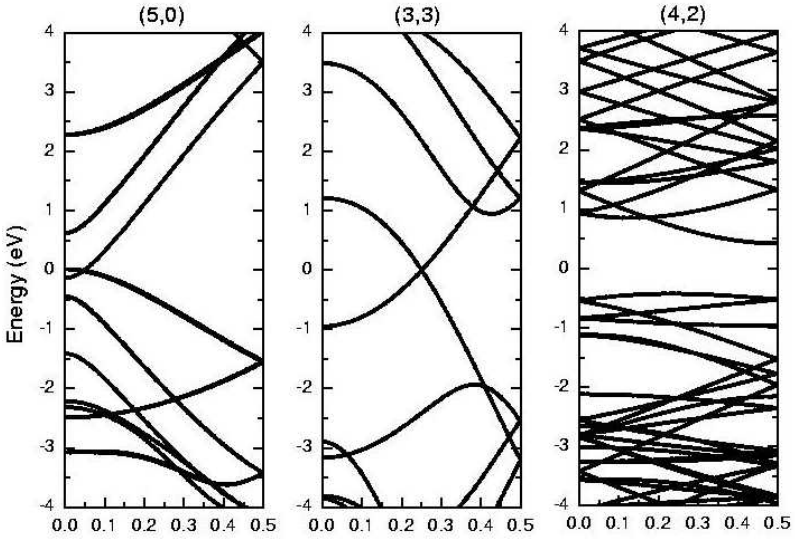

Fig. 1. Calculated electronic band structure of SWNTs (5,0), (3,3), and (4,2) in the energy range between –4 eV and 4 eV with respect to the Fermi energy.

Here, the structure of all 48 SWNTs with radii R in the range from 2 Å to 5 Å was optimised. The optimisation was carried out under the constraint that all atom lie on a cylindrical surface and as independent structural parameters were considered R, T, φ', and t'. The electronic band structure and the imaginary part of the dielectric function for parallel and perpendicular light polarisation were calculated for all mentioned SWNTs. In Fig. 1, the electronic band structure of three small-radius nanotubes, (5,0), (3,3), and (4,2), is shown. In all three cases, the predicted band structure corresponds semiquantitatively to the results in Refs. [18,19]. In particular, the expected large σ^*–π^* rehybridisation in thin tubes due to curvature effects [10] is demonstrated here as in Refs. [18,19]: the (5,0) nanotube is metallic contrary to the predictions of π-TB (ZFA); the crossing of the bands at the Fermi level in (3,3) nanotube is at $k \approx 0.25\ \pi/T$ instead at $k = 2/3\ \pi/T$; nanotube (4,2) has an indirect band gap of ≈0.83 eV which is twice smaller than the direct gap of the π-TB (ZFA) but is larger than the ab-initio one [18,19]. The effects of rehybridisation are found to decrease with the increase of the tube radius and to become unimportant for R close to 5 Å.

The calculated imaginary part of the dielectric function of SWNTs (5,0), (3,3), and (4,2) for parallel and perpendicular polarisation in the energy range from 0 to 6 eV are shown in Fig. 3. The peaks in parallel polarisation originate from minima and maxima of occupied and unoccupied bands with the same quantum number l. For example, peak A1 in Fig. 1 (tube (3,3)) can be associated with an optical transition between a maximum of an occupied band of ~ –2 eV and a minimum of an unoccupied band of ~1 eV. These minima and maxima give rise to spikes in the electronic density of states of the SWNTs.

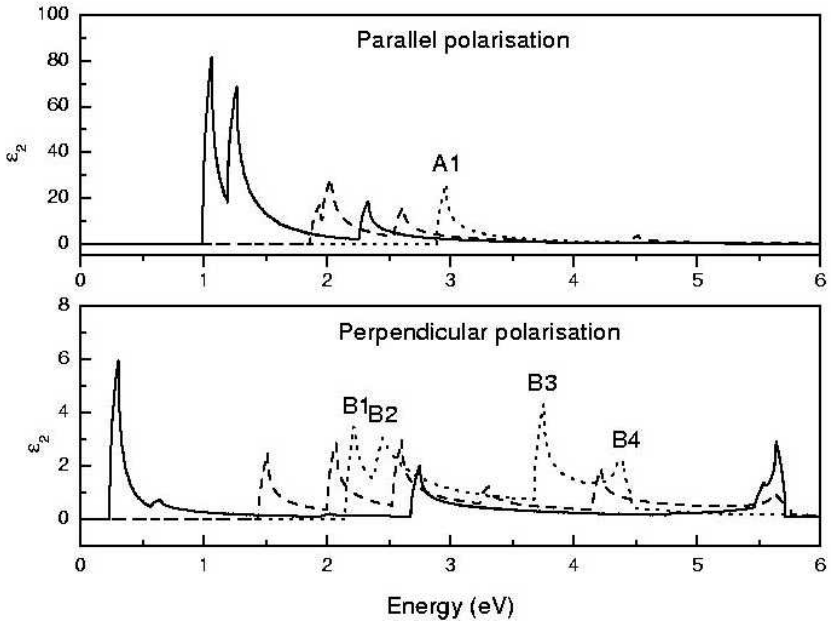

The peaks in perpendicular polarisation originate from minima and maxima of occupied
Fig. 2. Calculated dielectric function ε_2 of SWNTs (5,0) (solid line), (3,3) (dotted line), and (4,2) (dashed line) for parallel and perpendicular polarisation in the energy range from 0 to 6 eV.

and unoccupied bands as well from states on parallel parts of occupied and unoccupied bands with quantum numbers l and $l\pm1$. For example, peaks B1 and B2 come from such transitions near the crossing point of the bands at the Fermi level; peak B3 comes from states near the Brillouin zone boundary; peak B4 is due to transitions between minima and maxima of bands at the zone centre. It should be noted that in the calculation of ε_2 for perpendicular polarisation, the local field effects were not accounted for here. On the other hand, the small lateral size of the nanotubes leads to strong depolarisation effect and to significant reduction of the dielectric function [13]. The precise inclusion of the local field effects is expected to lead to improvement of the dielectric function for perpendicular polarisation mainly in the peak height. The importance of the knowledge of the dielectric function for both parallel and perpendicular polarisation has been stressed recently in a cross-polarised resonant Raman study of SWNTs [24].

The energies of the optical transitions in nanotubes determine the conditions for resonant Raman scattering of light from nanotubes. Previous results for these energies versus tube radius were derived within a π-TB (ZFA) [6]. In view of the inadequacy of these results for small-radius tubes it is important to correct them taking into account the curvature effects. Here, we present the transition energies versus tube radius for all 48 tubes with radii between 2 Å and 5 Å (Fig. 3). It is seen in Fig. 3 that as a result of curvature-induced hybridisation effects the nanotubes, predicted to be metallic within the π-TB (ZFA), are small-gap semiconducting tubes except for the armchair tubes that are always metallic due to their symmetry. In both metallic and semiconducting nanotubes, the energy bands come lower thus decreasing the energy of the optical transitions. These differences are large for very-small-radius nanotubes and tend to disappear for radii close to 5 Å.

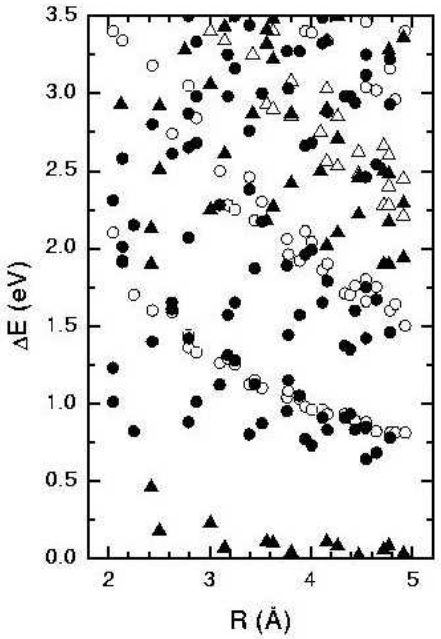

Fig. 3. Calculated optical transitions versus tube radius for parallel polarisation for all 48 tubes with radii between 2 Å and 5 Å in comparison with π-TB (ZFA) results from Ref. [6]. The circles denote semiconducting tubes and the triangles denote metallic tubes (according to the π-TB (ZFA)); open symbols are data from Ref. [6] and solid symbols are results obtained here.

3. Conclusions

The optical properties of single-walled carbon nanotubes (SWNTs) are studied within a density-functional-theory-based non-orthogonal tight-binding model. The model is symmetry-adapted which allows for significant reduction of the size of the matrix electronic eigenvalue problem. It is shown that the calculated electronic band structure of three small-radius nanotubes agrees well with ab-initio simulations up to several eV above the Fermi energy and exhibits large differences with the π-TB (ZFA) results. For example, nanotube (5,0) is found to be metallic while the π-TB (ZFA) predicts it as semiconducting. Secondly, the dielectric function for the same nanotube types is calculated within the random phase approximation for energies up to 7 eV. The obtained peak positions of the imaginary part of the dielectric function versus nanotube radius can be useful for determination of the conditions for resonant Raman scattering from nanotubes.

Acknowledgments

This work was supported partly by a NATO Senior Fellowship, the University of Antwerp (RUCA) - Belgium in the framework of the Visiting Professors Program, and the Flemish Region-IWT. The author acknowledges stimulating discussions with L. Henrard and A. Rubio.

References

1. S. Iijima, Nature (London) 354, 56 (1991).
2. M. S. Dresselhaus, G. Dresselhaus, and P. C. Eklund, Science of fullerenes and carbon nanotubes (Academic Press, New York, 1996).
3. R. Saito, G. Dresselhaus, and M. S. Dresselhaus, Physical properties of carbon nanotubes (Imperial College Press, London, 1998).
4. Carbon nanotubes: Synthesis, Structure, Properties, and Applications, edited by M. S. Dresselhaus, G. Dresselhaus, and Ph. Avouris (Springer-Verlag, Berlin, 2001).
5. R. Saito, M. Fujita, G. Dresselhaus, and M. S. Dresselhaus, Electronic structure of graphene tubules based on C60, Phys. Rev. **B 45**, 6234 (1992).
6. H. Kataura, Y. Kumazawa, Y. Maniwa, I. Umezu, S. Suzuki, Y. Ohtsuka, and Y. Achiba, Optical properties of single-wall carbon nanotubes, Synth. Metals **103**, 2555 (1999).
7. A. Hagen and T. Hertel, Quantitative Analysis of optical spectra from individual single-wall carbon nanotubes, Nano Letters **3**, 383 (2003).
8. N. Hamada, S. Sawada, and A. Oshiyama, New one-dimensional conductors: graphitic microtubules, Phys. Rev. Lett. **68**, 1579 (1992).
9. J. W. Mintmire, B. I. Dunlap and C. T. White, Are fullerene tubules metallic? Phys. Rev. Lett. **68**, 631 (1992).
10. X. Blase, L. X. Benedict, E. L. Shirley, and S. G. Louie, Hybridization effects and metallicity in small radius carbon nanotubes, Phys. Rev. Lett. **72**, 1878 (1994).
11. J.-C. Charlier, Ph. Lambin, and T. W. Ebbesen, Electronic properties of carbon nanotubes with polygonized cross section, Phys. Rev. **B 54**, R8377 (1996).
12. S. Reich, C. Thomsen, and P. Ordejón, Electronic band structure of isolated and bundled carbon nanotubes, Phys. Rev. **B 65**, 155411 (2002).
13. H. Ajiki and T. Ando, Aharonov-Bohm effect in carbon nanotubes, Physica **B 201**, 349 (1994).
14. M. F. Lin and K. W.-K. Shung, Plasmons and optical properties of carbon nanotubes, Phys. Rev. **B 50**, 17744 (1994)
15. S. Tasaki, K. Maekawa, and T. Yamabe, π-band contribution to the optical properties of carbon nanotubes: effect of chirality, Phys. Rev. **B 57**, 9301 (1998).
16. I. Milošević, T. Vuković, S. Dmitrović, and M. Damnjanović, Polarized optical absorption in carbon nanotubes: a symmetry-based approach, Phys. Rev. **B 67**, 165418 (2003).
17. J. W. Mintmire and C. T. White, Electronic structure simulations of carbon nanotubes, Synth. Metals **77**, 231 (1996).
18. Z. M. Li, Z. K. Tang, H. J. Liu, N. Wang, C. T. Chan, R. Saito, S. Okada, G. D. Li, J. S. Chen, N. Nagasawa, and S. Tsuda, Polarized absorption spectra of single-walled 4 Å carbon nanotubes aligned in channels of an AlPO4-5 single crystal, Phys. Rev. Lett. **87**, 121401 (2001).
19. M. Machón, S. Reich, C. Thomsen, D. Sánchez-Portal, and P. Ordejón, Ab-initio calculations of the optical properties of 4-Å-diameter single-walled nanotubes, Phys. Rev. **B 66**, 155410 (2002).
20. V. N. Popov, V. E. Van Doren, and M. Balkanski, Lattice dynamics of single-walled carbon nanotubes, Phys. Rev. **B 59**, 8355 (1999); V. N. Popov, V. E. Van Doren, and M. Balkanski, Elastic properties of single-walled carbon nanotubes, Phys. Rev. **B 60**, 3078 (2000).
21. D. H. Robertson, D. W. Brenner, and J. W. Mintmire, Energetics of nanoscale graphitic tubules, Phys. Rev. **B 45**, 12592 (1992).
22. H. Ehrenreich and M. H. Cohen, Self-consistent field approach to the many-electron problem, Phys. Rev. **115**, 786 (1959).
23. D. Porezag, Th. Frauenheim, and Th. Köhler, Construction of tight-binding-like potentials on the basis of density-functional theory: application to carbon, Phys. Rev. **B 51**, 12947 (1995).
24. A. Jorio, M. A. Pimenta, A. G. Souza Filho, Ge. G. Samsonidze, A. K. Swan, M. S. Ünlü, B. B. Goldberg, R. Saito, G. Dresselhaus, and M. S. Dresselhaus, Resonance Raman spectra of carbon nanotubes by cross-polarized light, Phys. Rev. Lett. **90**, 107403 (2003).